*Pak. J. Engg. Appl. Sci. Vol. 22 January*, 2018 (*p.* 72–80)

# Laboratory Modelling and Assessment of Internal Instability Potential of Subballast Filter under Cyclic Loading

Jahanzaib Israr[1] and Jehangir Israr[2]

1. *Department of Civil Engineering, University of Engineering and Technology, Lahore, Pakistan*
2. *Water and Sanitation Agency (WASA), Lahore Development Authority (LDA), Pakistan*

* **Corresponding Author:** Email: ji797@uowmail.edu.au

## Abstract

*Internal instability occurs when the flow under the influence of seepage forces washout the finer fraction from granular soils, resulting in the deterioration of the mechanical and geotechnical properties, e.g. change in soil gradation, large volumetric strains and increased permeability etc. In railway substructures, filters are installed as drainage or subballast layers to arrest the eroding subgrade fines into superstructure that could otherwise endanger the stability of tracks due to ballast fouling and clay pumping. Notably, the design and assessments for internal instability potential for subballast are currently emphasized through existing filtration criteria which neglect the effects of cyclic loading. This paper reports an investigation of the internal stability assessment of saturated subballast filters subjected to cyclic loading. Experimental results conducted on selected soil gradations in specially designed cyclic loading permeameter revealed that repeated loading promotes substantial and premature suffusion failure, the intensity of which increases with the loading frequency. An existing criterion for assessing the internal instability potential is modified to capture the effects of cyclic loading that is subsequently validated through extensive laboratory data. Comparisons between static and cyclic response of test samples revealed that the suffusion could occur at unique hydro-mechanical boundaries, which would have implications in practical design of internally stable subballast filters under unfavorable hydro-mechanical and cyclic loading conditions.*

**Key Words:** Subballast; Cyclic Loading; Seepage; Internal Instability; Hydraulic Gradient; Relative Density; Pore Pressure.

## 1. Introduction

In railway substructures, the subballast layer performs two major functions, namely (i) preventing the ballast from making direct contact with the subgrade during load transfer, and (ii) avoiding the upward movement of subgrade fines into upper layers induced by pore pressure. Direct contact between ballast and subgrade may lead to natural subgrade particles being crushed and intermixing with the ballast and subgrade soils; this results in extensive subgrade particle attrition and the layer of ballast penetrating the subgrade soils, promoting progressive shear failure. A properly designed subballast filter can prevent intermixing with the ballast and pumping of subgrade particles, and thus safely dissipate pore pressure developing in the subgrades. However, uniform gravels may be too coarse to capture the eroding subgrade fines (generally < 0.15 mm), while uniform fine sands could be susceptible to the development of high pore pressure. Given that subballast also serves as a capping layer to transfer loads from the ballast to the foundation, it must have a durable particle fabric that is insensitive to variations in moisture and enough permeability to avoid the build-up of pore pressure due to cyclic loads [1]. An abrasion resistant and internally stable sand-gravel mixture selected through well-accepted filter design criteria can possibly meet these requirements.

The flow through subballast is impulsive, which mainly stems from the development of excess pore water pressure in subgrade soil during train operations. However, there is very limited information available in literature regarding the magnitude of hydraulic pressure generated that may significantly vary with the in situ conditions such as train speed (frequency), loading magnitude, soil characteristics and confining pressures etc. [1,2]. Furthermore, simulating field conditions in the laboratory including pore water pressure development under cyclic loading that would also induce flow through filter is not yet very well understood. In this study, the authors simulated flows at hydraulic gradients in excess of 50, which may adequately represent extreme flow conditions. Nevertheless, the hydraulic pressures were increased in controlled steps and each step itself represented an impulsive flow through filters.

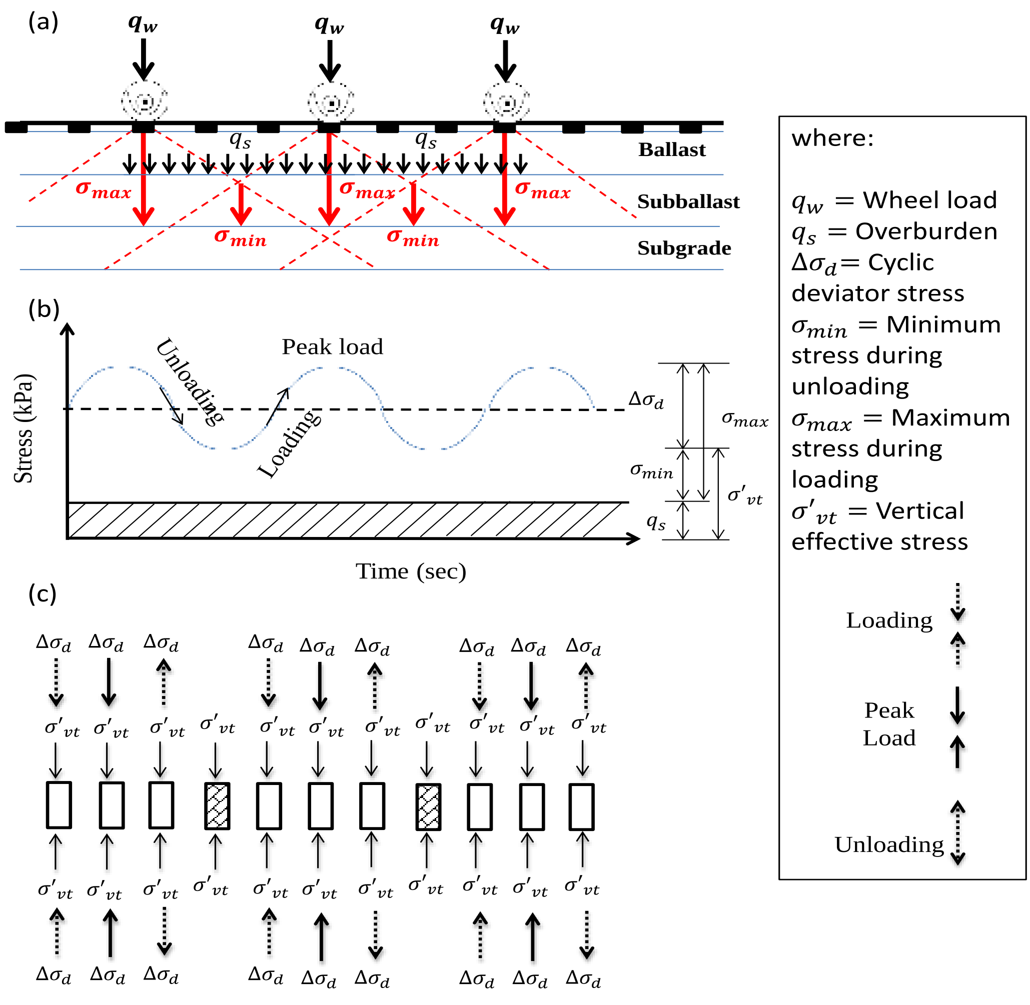


**Figure 1:** Illustration of mechanical load and stress transfer mechanisms in railway substructure

The internal stability of soils is assessed through various particle size distribution (PSD) based criteria that were established based on observations from laboratory hydraulic tests under static conditions, and with and without imparting the vibrations during testing [3, 4, 5, 6]. The occurrence of instability changes the soil gradations that consequently deteriorate the mechanical and geotechnical properties, i.e. large volumetric strains and increased permeability, etc. Reportedly, these criteria conservatively differentiate between stable and unstable soils such that internal instability is then believed to be exhibited only by the latter [7].

However, under cyclic conditions, geometrically assessed internally stable gradations reportedly exhibit premature suffusion of their skeletal fines, like unstable soils [2]. In this study, hydraulic tests were carried out to obtain a science based explanation of the above discrepancy between the static and cyclic response of selected subballast soil gradations that are typically used in railway foundation in New South Wales (NSW), Australia. Based on the test results, an existing criterion for assessing the instability potential of soils is modified to capture the effects of cyclic loading. Comparisons between static and cyclic hydraulic tests revealed that suffusion occurs at unique hydro-mechanical boundaries that would have implications in practical filter design [3, 10, 11].

## 1.1 Geometrical Criteria of Internal Stability Assessments

Kezdi [5] proposed to split the PSD curve at an arbitrary point to obtain an idealized system of base and filter soils. For brevity, the method determines the maximum value of ($D_{15}/d_{85}$), where D15 and d85 represent the controlling particle sizes for the idealized filter and base soils, respectively. An internally stable soil would satisfy the criterion of Terzaghi [10], i.e. ($D_{15}/d_{85}$) $\leq$ 4, while a more relaxed condition of ($D_{15}/d_{85}$) $\leq$ 5 was proposed by Sherard [6].

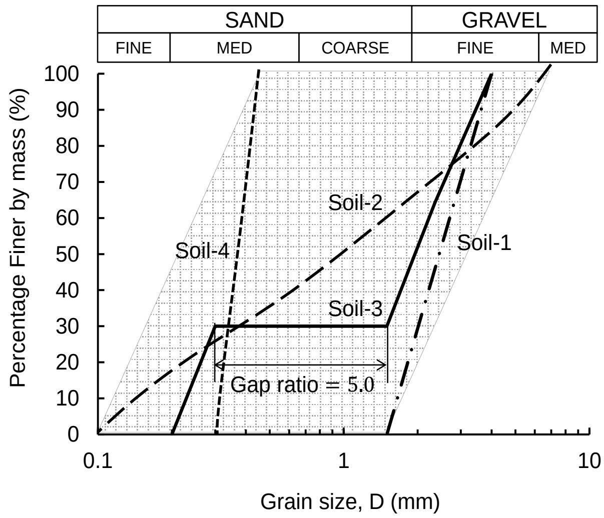


**Figure 2:** Particle size distribution curves for current test specimens

Kenney and Lau [4] proposed that an arbitrary soil particle d on the PSD curve can erode through a constriction formed by the particles larger than or equal to 4d, whereas the particle sizes within the range of d and 4d may significantly reduce the potential of erosion The above condition could be represented in the form of ratio $(H/F)_{min}$, where H and F represent the percentage passing by mass between particle sizes *d* and *4d*, and that corresponding to the size *d*, respectively.

Given that the CSD is a combined function of PSD and relative density ($R_d$), based on which variety of constrictions are formed within the granular media [11, 12]. The fines eroded through one constriction may be captured by another, i.e. localized self-filtering. Similarly, the percentage of finer fraction (F) controls the potential of instability of soil, for which Kenney and Lau [4] assumed that the erodible particles exist in the loose state in the soil and proposed the upper limits of F subject to erosion for soils with $C_u > 3$ and $C_u \leq 3$ as 20% and 30%, respectively.

Indraratna et al. [3] proposed that the PSD curve of a given soil is demarcated at a point corresponding to $(H/F)_{min}$ value to idealize a coarser (filter) and a finer (base) fraction. The controlling constriction size of filter $D_{c35}$ at 35% finer and the characteristic particle size of base $d_{f85}$ at 85% finer by surface area are determined. A soil possessing $(D_{c35}) / (d_{f85}) \leq 1$ would be characterized as internally stable. Unlike traditional PSD based criteria, geometrical methods, the CP-CSD method is sensitive to both PSD and $R_d$ of soil.

## 2. Experimental Program

A series of 20 seepage induced piping tests were conducted on four different soil gradations under static and cyclic loading conditions. The basic objective of static piping tests is to determine the exact internal instability potential for all four soils and then compare them with the results of cyclic tests. Under static conditions, hydraulic tests were conducted under two different scenarios, namely (i) under the self-weight of specimens only (i.e. $\sigma'_{vt} = 0$) and, (ii) under $\sigma'_{vt} =$ 50 kPa. The cyclic tests were conducted under typical heavy haul freight loading in NSW (i.e. $\sigma'_{min} = 30$ kPa and $\sigma'_{max} = 70$ kPa) to simulate loading and unloading cycles [2, 13, 14] (Figure 1). Cyclic tests were divided into four main categories, namely tests under sinusoidal cyclic loading frequency where $f =$ (i) 5 Hz, (ii) 10 Hz, (iii) 15 Hz, and (iv) 20 Hz.

### 2.1 Test Material and Specimens

Figure 2 shows the particle size distribution (PSD) curves of soil specimens tested in this study. The shaded area represents the typical range of subballast filter selection currently being practiced in Australia [8, 14, 15, 16, 17].

In Australia, the natural material for subgrade may contain silt, clay or their mixtures (0.0018mm to 0.07mm). The material for subballast would comprise of sands (SP and SW) and gravels (GP and GW) with maximum particle size of 25mm (Figure 2). The material for ballast consists of crushed basaltic rock (GP and GW) with particle sizes ranging between 9mm and 45mm [18, 19]. The test specimens consisted of uniform fine gravels (Soil-1), broadly-graded gravelly-sand (Soil-2), gap-graded sand-gravel mixture (Soil-3), and uniform fine sand (Soil-4). For soils 1, 2, 3, and 4, the Unified Soil Classification System classified as GP, GW, SW, and SP, respectively, while the AASHTO classification system characterised s as A-1-a, A-1-b, A-1-a, and A-3, respectively. A number of well-accepted existing criteria were applied to assess the internal instability potential for current soil gradations. The PSD based criteria established soils-1 and -4 as stable and soils-2 and -3 as unstable, while the constriction size distribution (CSD) based approach of [4] assessed soils-1, 2, and 4 as stable and soil-3 as unstable.

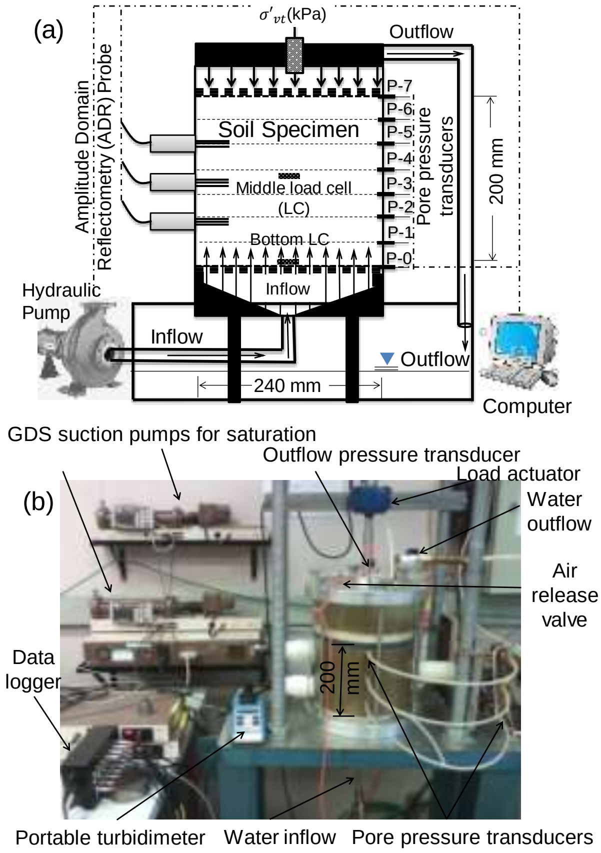


**Figure 3:** Illustration of test apparatus and setup

These soils do not just cover the typical selection range of subballast (shaded area in Fig. 2) but also form a blend of potential internally stable and unstable soils. Notably, the current soil 3 was tested with a twofold objective, namely; (1) to represent an already existing subballast layer, i.e. intermixed with the subgrade particles [2], and (2) to compare the seepage induced response of internally unstable gap-graded soil with that of stable uniform and marginal well-graded soils for the possible recommendations of their use in practice.

The specimens for testing were prepared at a maximum relative density (i.e. $R_d \geq 95\%$) but for brevity, the approach used by Indraratna et al. [3] for preparing specimens was adopted, including compaction, saturation, and assessing the uniformity of specimens with respect to particle size distribution and compaction. For brevity, the soils were mixed beforehand and compacted in 5 different layers to obtain 0.2m long specimens at target relative density by controlling the soil mass for the given volume and the limiting void ratios $e_{min}$ and $e_{max}$. The uniformity of test specimens with regards to particle size distribution and compaction was examined through additional tests. The uniformity with respect to compaction was assessed by measuring the overall density as well as the densities of the small specimens cored within the test samples. Similarly, the uniformity with respect to particle gradation was examined through pre-test and post-test PSD analysis results. The specimens were then carefully saturated with filtered water after de-airing under a high back pressure of 120 kPa for an extended period of 24 to 48 hours.

## 2.2 Test Apparatus and Procedure

Figure 3 shows the test apparatus; it consisted of a 240 mm diameter low-friction (Teflon coated) polycarbon cell that could accommodate a 200 mm long specimen (Fig. 2). Due to the cell dimensions yielding sufficient size ratios (i.e. $500 > d/D_{100} > 25$, where d = cell diameter and $D_{100}$ = largest particle size), the effects of boundary friction and preferential flow on particle erosion could be minimized to an acceptable level [20]. Arrays of 8 pore pressure transducers, 3 amplitude domain reflectometry (ADR) probes, and 3 load cells each at top, middle, and bottom, i.e. 150mm, 100mm and 50mm from the base of hydraulic cell, respectively were installed inside each test specimen to monitor the seepage induced local hydraulic gradients, porosity, and effective variations in stress.

During testing the saturated samples were subjected to an upward flow of water at pre-requisite hydraulic pressure levels (hence an average hydraulic gradient of $i_a$). The $i_a$-values were increased at a controlled rate, e.g. increment rates of $\Delta i_a =$ 0.05 and 0.025 per 30 minutes were adopted for potential internally stable soils (soils-1 and -4) and unstable soils (soils-2 and –3), respectively. Effluent turbidity, axial strain, and the total loss of mass due to erosion were also captured as additional parameters. For instance, the washed out fines were measured through the post-test forensic analysis of the material captured in the effluent collection tank. The percentage of erosion could also be deduced from the difference between pre-test and post-test PSD curves of tested soils for comparison with measured erosion and no significant difference was recorded. The tested specimens were retrieved in 3 distinct layers (top, middle, and bottom) and a PSD analysis was carried out to compare the changes between pre- and post-test specimens to quantify their internal stability.

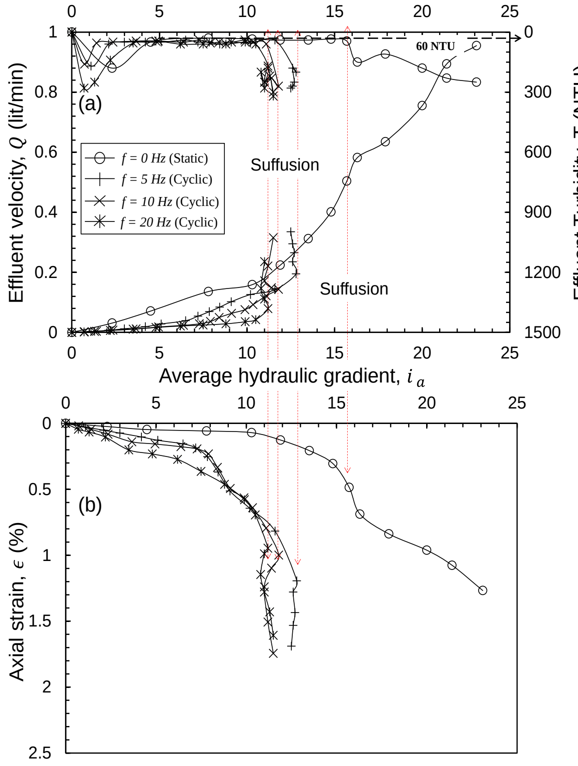


**Figure 4:** Hydraulic test results for soil-3 (a) flow curves and turbidity variations (b) axial strain evolution with the applied hydraulic gradients

## 3. Test Results and Discussions

Figure 4 shows the results of hydraulic tests for soil-3, including flow curves (i.e. correlations between the applied hydraulic gradients and effluent flow rates *Q*), variations in seepage induced turbidity, and evolutions of axial strain. The inception of internal instability could be characterized by a significant increase in *Q* (lit/min) indicated by a sudden change in the slope of flow curves, while the effluent turbidity became much greater than 60 NTU [3]. The corresponding average (Eq. 1) and local hydraulic gradient (Eq. 2) values were measured as the critical hydraulic gradients ($i_{cr,a}$ and $i_{cr,ij}$ respectively).

$$i_a = \frac{p_w^{in} - p_w^{out}}{h_f \times \gamma_w} \tag{1}$$

$$i_{ij} = \frac{p_w^{(i+1)(j+1)} - p_w^{ij}}{\Delta y \times \gamma_w} \tag{2}$$

Where $p_w^{in}$ and $p_w^{out}$ define the inflow and out flow hydraulic pressures across the whole sample depth ($h_f$), respectively, while $p_w^{(i+1)(j+1)}$, and $p_w^{ij}$ define the inflow and outflow pressures across a layer of soil ($\Delta y$), respectively.

Notably, there is no significant difference between the terms average and local hydraulic gradients except for the depth of soil layer. The average hydraulic gradient is measured for the total depth of soil layer, whereas the local hydraulic gradient refers to a discrete depth of soil. Nevertheless, the local hydraulic gradient may provide more accurate information regarding the inception of instability in soils.

Under static conditions the results of the hydraulic test revealed that soil-1, -2, and -4 exhibited heave development at much higher magnitudes of applied hydraulic pressure and were therefore deemed internally stable. For tests under self-weight, heave in the above specimens occurred at hydraulic gradients ≥ 1.0 and showed closer agreements with the classical piping theory of Terzaghi [10]. For tests where $\sigma'_{vt} = 50$ kPa, the magnitudes of effective stresses continued to decrease as the hydraulic pressure increased, and heave initiated at very small magnitudes of effective stresses (i.e. ≤ 10 kPa).

The results of the post-test PSD analysis revealed that the gradations of the central portions of these specimens did not alter after testing, which also confirmed the internal stability of soils-1, -2, and -4. However, soil-3 exhibited a marked suffusion of its finer fraction at relatively smaller hydraulic gradients and therefore it is deemed internally unstable; the post-test PSD analysis also confirmed this observation. Notably, the magnitude of effective stress was still > 40 kPa when suffusion occurred which clearly indicated that a significant portion of fines were not fully participating in the sustainable stress transfer and were therefore bearing relatively lower magnitudes of effective stresses [21]. Nevertheless, the washout of fines from soil-3 increased with an increase in the hydraulic pressure, and that resulted in an increase in the axial strain rate (i.e. settlement), indicating the test specimen experienced progressive shear failure (Figure 4).

Under cyclic conditions, the response of soil-1 was almost similar to that under static piping tests, whereby heave occurred at very high applied hydraulic gradient and the post-test PSD analysis revealed that it was internally stable at all loading frequencies. Soil-4 exhibited piping failure instead of heave at hydraulic gradients equivalent to those observed during static piping tests with relatively higher axial strain and turbidity under cyclic loading. The post-test PSD analysis revealed no significant variation in PSD curves in the central portion, and therefore soil-4 was also deemed to be internally stable at all loading frequencies. The internally unstable soil-3 again showed that its finer fraction had washed out at smaller hydraulic gradients, and that became excessive as the loading frequencies increased. The response of soil-2 was dramatic under cyclic loading, because it showed excessive suffusion under all hydraulic tests with higher mass loss and subsequently higher axial strain rates as the loading frequency increased. The washout initiated at increasingly smaller magnitudes of hydraulic gradients and at higher stress levels indicated that the increasing loading frequency imparted higher disturbance to the granular media due to agitation. Figure 6 shows the selected test specimens and their seepage induced response under static and cyclic conditions during testing.

## 4. Assessing the Potential of Internal Instability

Several well-known existing PSD [4, 5, 6] and CSD [3] based approaches were used to assess the potential of current test gradations for internal instability, and the results are summarized in Table 1. As described previously, all the existing criteria correctly assessed the internal instability potential under static conditions, but none of these criteria could correctly capture the stability potential for soil-2 which showed internal instability in all hydraulic tests conducted under cyclic loading conditions. In summary, soils-1, -2, and -4 were experimentally assessed as being stable during static piping tests, while soil-3 was deemed to be internally unstable.

On the other hand, soils-1 and -4 were found to be stable and soils-2 and -3 were unstable under cyclic loading conditions. Interestingly, the seepage induced response for soil-2 at $R_d \geq 95\%$ under cyclic loading was found to be identical to that of a geometrically similar specimen C-20 of Indraratna et al. [3] at $R_d \approx 0\%$ under static conditions. A probable explanation would be that the constriction network of soil-2 continued to deteriorate as the loading frequency increased and this allowed more fines to erode, as indicated by the post-test PSD analysis (Figure 5).

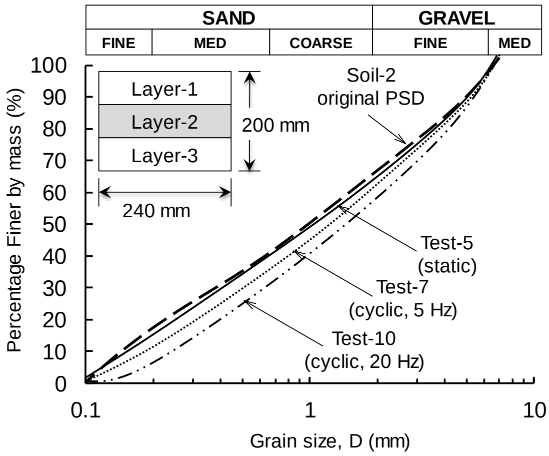


**Figure 5**: Post-test PSD analysis results for soil-2 under static and cyclic loading (Test numbers in Table 1)

### 4.1 Proposed Method

The hydraulic excitation in railway substructures mainly stems from the pore water pressure developed due to cyclic loading. Therefore, to compensate for the effects of agitation, it is proposed here to assume that the layer of subballast filter possesses minimum relative density (i.e. $R_d = 0\%$) under cyclic loading condition. Given that the pore constrictions can only vary between the limits of densest and loosest constriction sizes [11], the above assumption will be more realistic because it captures the worst case of loosest constriction sizes.

As discussed in the previous section, the criteria of Kenney and Lau [4], Kezdi [5], and Sherard [6] showed the highest success rates for correctly assessing the potential of internal instability of soils. The proposed hypothesis of $R_d = 0\%$ was used in conjunction with the criterion of Indraratna et. al. [3] to assess the potential of internal instability, and the results are reported in Table 1. It can be clearly seen that the proposed method captures the correct potential for internal instability for current test specimens with 100% success.

## 5. Hydromechanical Boundary for Internal Instability

Figure 7 shows the correlation between magnitudes of local hydraulic gradients (Eq. 2) in the discrete soil layers where internal instability initiated and the companion values of effective stresses. Variations in the magnitude of effective stresses were monitored by three load cells, i.e. one each placed at the top, middle, and bottom of the test specimens. Assuming a linear stress distribution, the magnitude of stress in a given layer of soil could be obtained from the load cell measurements.

As shown, the results from all the static and cyclic piping tests were plotted together and the local critical hydraulic gradient could be correlated with the effective stress magnitudes with a unique correlation. Due to similar initial stress conditions for all these tests (i.e. the applied top stress $\sigma'_{vt}$ = 50 kPa for static and the mean applied cyclic stress $\sigma'_{vm} \approx$ 50 kPa for cyclic tests), a unique envelope could be obtained when the values of $i_{cr,ij}$ and $\sigma'_{v}$ were plotted. Given that only a single heavy-haul loading was simulated in this study, the hydro-mechanical envelope is likely to vary with the loading conditions. Nevertheless, these correlations may have implications in the practical design of filters under unfavorable conditions, including cyclic loading; although the concept of a hydro-mechanical model is premature at this stage.

## Concluding Remarks

In this study, laboratory hydraulic tests were conducted under static and cyclic loading conditions at the Hi-Bay laboratory of University of Wollongong Australia to evaluate the factors governing the potential and the inception of internal instability in granular filters. Based on the analysis of test results, the following conclusions were drawn:

The broadly-graded and gap-graded soils exhibit greater tendencies to suffer from internal instability under cyclic conditions, therefore their use as subballast filter must be avoided.

It was observed that the cyclic loading promoted premature suffusion and piping failures in internally unstable soils and stable uniform sands, respectively, and this resulted in higher axial strain rates and settlements compared to those under static conditions.

**Table 1:** Summary of laboratory test results

| **Test No.** | **Sample ID** | ***f* (Hz)** | **Internal stability assessment** | | | | | | **€ (%)** | **T (NTU)** |
|---|---|---|---|---|---|---|---|---|---|---|
| | | | **I** | **KL** | **K** | **S** | **CM** | **Experimental** | | |
| 1 | Soil-1 | 0 | S | S | S | S | S | S | 0.05 | 0 |
| 2 | | 0* | S | S | S | S | S | S | 0.01 | 0 |
| 3 | | 5 | S | S | S | S | S | S | 0.02 | 48 |
| 4 | | 20 | S | S | S | S | S | S | 0.025 | 55 |
| 5 | Soil-2 | 0 | S | S | S | S | S | S | 0.82 | 50 |
| 6 | | 0* | S | S | S | S | S | S | 0.9 | 42 |
| 7 | | 5 | S | S | S | S | U | U | 1.12 | 88 |
| 8 | | 10 | S | S | S | S | U | U | 1.22 | 104 |
| 9 | | 15 | S | S | S | S | U | U | 1.28 | 120 |
| 10 | | 20 | U | U | U | U | U | U | 1.34 | 140 |
| 11 | Soil-3 | 0 | U | U | U | U | U | U | 1.17 | 155 |
| 12 | | 0* | U | U | U | U | U | U | 1.24 | 195 |
| 13 | | 5 | U | U | U | U | U | U | 1.62 | 200 |
| 14 | | 10 | U | U | U | U | U | U | 1.68 | 255 |
| 15 | | 15 | U | U | U | U | U | U | 1.75 | 270 |
| 16 | | 20 | U | U | U | U | U | U | 1.71 | 250 |
| 17 | Soil-4 | 0 | S | S | S | S | S | S | 1.07 | 130 |
| 18 | | 0* | S | S | S | S | S | S | 1.18 | 145 |
| 19 | | 5 | S | S | S | S | S | S | 1.27 | 170 |
| 20 | | 20 | S | S | S | S | S | S | 1.38 | 185 |

**Note:** f, €, T, S, and U define cyclic loading frequency, axial strain, turbidity, stable, and unstable, respectively. The acronyms I, KL, K, S, and CM represent criteria of Indraratna et al. [4], Kenney and Lau [4], Kezdi [5], Sherard [6], and the current method, respectively.

* Tests without instrumentation

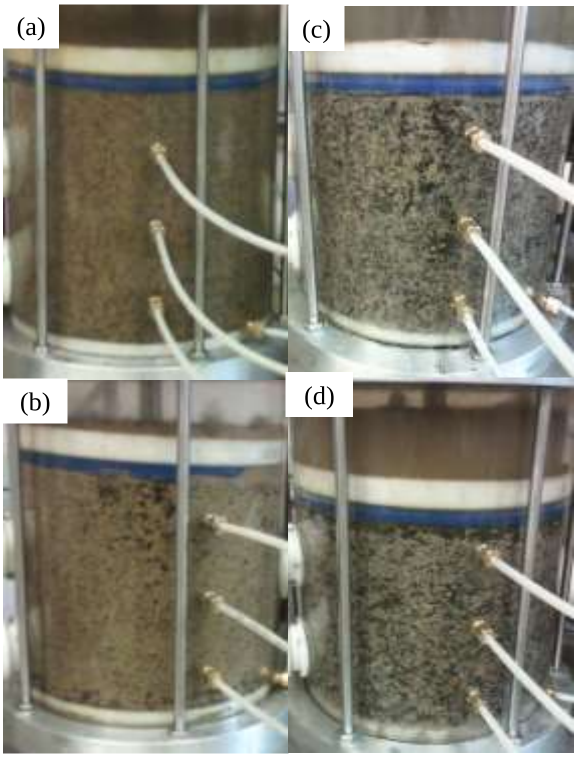


**Figure 6:** Illustrations of (a) Soil-2 under static piping test, (b) Initiation of heave in soil-2, and (c) excessive washout from soil-2 under cyclic loading at 15 Hz, and (d) excessive washout in soil-3 under cyclic loading.

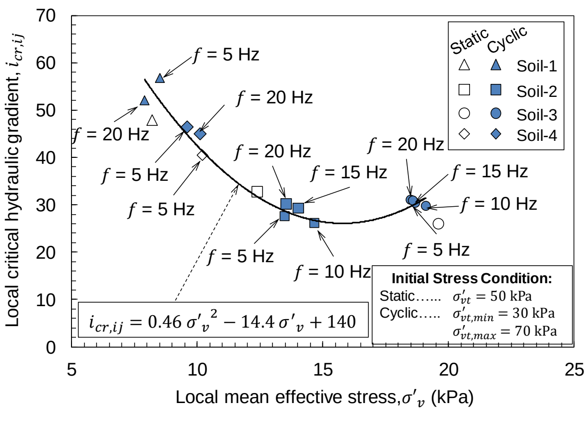


**Figure 7:** A hydro-mechanical correlation observed between local hydraulic gradients and effective stress magnitudes for current test results.

The cyclic loading imparted significant agitation to the granular media and caused marked deteriorations in its constriction sizes, thereby allowing more erosion than under static conditions. Several existing methods were tested to assess the correct potential of internal instability of tested soils but they could not correctly capture the above effects of cyclic loading.

To account for agitation due to cyclic loading, it was proposed to assume zero relative density of soil when obtaining the CSD of a coarse fraction for quantifying its capacity to retain the finer fraction. This hypothesis was subsequently validated against the current test results and 100% success was obtained.

For the heavy-haul loading simulated in this study, a unique hydro-mechanical envelop appeared between the local hydraulic gradients and companion effective stresses. This correlation may have implications in practical filter design for unfavorable conditions such as cyclic train loading.

As part of obvious limitations, the proposed geometrical criterion is dependent on the particle size distribution of soils. Similarly, the idea of hydro-mechanical modelling is premature at this stage and the authors do envisage expanding this concept to more practical conditions to formulate a hydro-mechanical approach for practical filter design. Given that the main objectives of this study included geometrical and hydraulic evaluations of internal instability potential of select soils; which is why the hydro-mechanical aspects were not covered in greater depth. Nevertheless, the most appropriate method to accurately determine the internal instability potential of soils is still the laboratory filtration test.

## Acknowledgement

The authors are grateful to the University of Engineering and Technology Lahore, Pakistan and University of Wollongong (UoW), Australia for awarding research funds to the first author in the form of Faculty Development Program and International Post-Graduate Tuition Award scholarships. The invaluable assistance of Hi-Bay laboratory technical staff of UoW in developing the test apparatus and conducting the testing is heartily acknowledged.

## References

[1] Selig, E. T., & Waters, J. M. (1994). Track technology and substructure management. Thomas Telford, London.

[2] Trani, L. D. O., & Indraratna, B. (2010). Assessment of Subballast Filtration under Cyclic Loading. Journal of Geotechnical and Geoenvironmental Engineering 136(11), 1519-1528.

[3] Indraratna, B., Israr, J., & Rujikiatkamjorn, C. (2015). Geometrical method for evaluating the internal instability of granular filters based on constriction size distribution. Journal of Geotechnical and Geoenvironmental Engineering 141(10), 1-14. (DOI: 10.1061/(ASCE)GT.1943-5606.0001343).

[4] Kenney, T. C., & Lau, D. (1985). Internal stability of granular filters. Canadian Geotechnical Journal 22, 215–225.

[5] Kezdi, A. (1979). Soil physics, Elsevier Scientific, Amsterdam, The Netherlands.

[6] Sherard, J. L. (1979). Sinkholes in dams of coarse broadly graded soils. In Proceeding of the 13th Congress on Large Dams, Paris, France, 1(2), 25–35.

[7] Li, M., & Fannin, R. J. (2008). Comparison of two criteria for internal stability of granular soil. Canadian Geotechnical Journal 45(9), 1303–1309.

[8] Israr, J., & Indraratna, B. (2017). Internal stability of granular filters under statc and cyclic loading. Journal of Geotechnical and Geoenvironmental Engineering 143(6) , 04017012 (DOI:10.1061/(ASCE)GT.1943-5606.0001661).

[9] Indraratna, B., Israr, J., & Li, M. (2017). Inception of geohydraulic failures in granular soils-an experimental and theoretical treatment. Geotechnique, 1-16 (DOI: 10.1680/jgeot.16.P.227)

[10] Terzaghi, K. (1939). Soil mechanics—A new chapter in engineering science. Institute of Civil Engineers 12(7), 106–142.

[11] Locke, M., Indraratna, B., & Adikari, G. (2001). Time-dependent particle transport through granular filters. Journal of Geotechnical and Geoenvironmental Engineering 52(6), 521-529.

[12] Israr, J., & Indraratna, B. (2018). Assessment of internal stability of filters under static and cyclic loading: an experimental and theoretical treatment. Australian Geomechanics Journal (In Press), 1-14.

[13] Israr, J., Indraratna, B., & Rujikiatkamjorn, C. (2016) Laboratory investigation of the seepage induced response of granular soils under static and cyclic loading. Geotechnical Testing Journal 39(5), 795-812.

[14] Israr, J., & Israr, J. (2018). Experimental investigation and assessment of internal stability of granular filters under one-dimensional static and cyclic loading. Geotechnical Testing Journal, 41(1), 103-116 (DOI: 10.1520/GTJ20170027. ISSN 0149-6115).

[15] Ip, C. M., Haque, A. & Bouazza, A. (2012). Influence of cyclic stress pulse shapes on filtration behaviour of railway subballast. Journal of Geotechnical and Geoenvironmental Engineering 138(2), 230-235.

[16] Haque, A., Kabir, E., & Bouazza, A. (2007). Cyclic filtration apparatus for testing subballast under rail track. Journal of Geotechnical and Geoenvironmental Engineering, 133(3), 338-341.

[17] Kamruzzaman, A. H. M., Haque, A., & Bouazza, A. (2008). Filtration behaviour of granular soils under cyclic load. Geotechnique 58(6), 517–522.

[18] Trani, L. D. O. (2009). Application of constriction size based filtration criteria for railway subballast under cyclic conditions. Ph.D. Thesis, University of Wollongong, Australia.

[19] Indraratna, B., Sun, Y., & Nimbalkar, S. (2016). Laboratory Assessment of the Role of Particle Size Distribution on the Deformation and Degradation of Ballast under Cyclic Loading. Journal of Geotechnical and Geoenvironmental Engineering 142(7), 04016016.

[20] Zou, Y., Chen, Q., Chen, X., & Cui, P. (2013). Discrete numerical modelling of particle transport in granular filters. Computers and Geotechnics, 32(5), 340–57.

[21] Skempton, A. W., & Brogan, J. M. (1994). Experiments on piping in sandy gravels. Geotechnique 44(3), 449–460.